"Physics of Auroral Phenomena", Proc. XXXVIII Annual Seminar, Apatity, pp. 40-43, 2015

Polar Geophysical Institute

THE SATURATION EFFECT OF THE POYNTING FLUX INTO THE MAGNETOSPHERE DURING SUPERSTORMS: RESULTS OF MIT AND THE GLOBAL PPMLR-MHD MODEL

V.V. Mishin[1], Yu. Karavaev[1], J.P. Han[2,3], C. Wang[3]

[1]*ISTP SB RAS, Irkutsk*
[2]*CALT CASC, Beijing, China,*
[3]*NSSC CAS, Beijing, China*

Abstract. We study the effect of the slowing growth of the polar cap magnetic flux and the electromagnetic energy flux into the magnetosphere from the solar wind (SW) during the superstorm significant strengthening. This saturation effect is found not only depending on the SW electric field E_{sw} and / or on the southward IMF component, but also on the SW dynamic pressure P_d. Analytically and numerically we have been shown the existence of another saturation effect− slowing the dayside magnetosphere compression upon reaching high values of P_d and negative Bz. The both saturation effects are supposed to be associated with each other for superstorm conditions.

Introduction

Two important parameters characterize the efficiency of the SW− magnetosphere coupling: the cross polar cap voltage U_{PC} and the polar cap magnetic flux Ψ. A large number of papers were devoted to the saturation effect of the polar cap potential U_{PC} and magnetospheric convection – slowing down their growth upon reaching high values E_{sw} (E_{sw}=3-5 mV/m) and its further increasing. This effect has been confirmed by various measurement techniques and modelling. U_{PC} reaches an upper limit or saturates for increasing of large Esw values [e.g. *Borovsky et al.*, 2009; *Kan et al.,* 2010; Lyatsky et al., 2010; *Gao et al.*, 2013]. *Merkin et al.* [2007] and *Lopez et al.* [2009] demonstrated that the polar cap magnetic flux also saturates (at around 1 GWb) as the polar cap potential saturates. Transpolar potential saturation is the limit on transpolar potential that corresponds to the ram-pressure limit on total region 1 current [*Siscoe et al.*, 2002]. Because during superstorms both E_{sw} and P_d reach unusually high values, there is a question about the influence of P_d on the saturation level during superstorms. However, all above studies including *Siscoe et al.* [2002] have not obtained the saturation effect depending on the SW dynamic pressure. *Merkin et al.* [2007] obtained the saturation as consequence of the nightside reconnection point motion towards the inner plasma sheet boundary. However, these authors as also *Siscoe et al.* [2002] supposed that the dayside magnetosphere can also play very important role in the saturation effect and wanted to study this possibility but did not do yet. This task was carried out in [*Karavaev et al.*, 2012 a, b], where by the method of magnetogram inversion technique (MIT) of ground-based magnetometers, we found the saturation effect of the polar cap magnetic flux, depending on the SW dynamic pressure P_d from data of the superstorms (24-25) September 1998 and 20 November 2003. In the present study, these results are generalized, involving also the (6-7) April 2000 superstorm data. In addition, we use the results of numerical modeling of the global PPMLR− MHD model of the magnetosphere for the 20 November 2003 superstorm. We compare the graphs of variations of the energy flux into the magnetosphere, depending on the SW parameters E_{sw}, B_z, and P_d obtained by the two methods.

Moreover, we carried out an analytical and numerical analysis of the dependence of the subsolar magnetopause point position, on P_d as well as on the southward IMF component. It is shown a presence of saturation effects, not only of the magnetic flux Ψ and the corresponding energy flux through the polar cap, but also of the dayside magnetopause position - the suspension of its compression at strengthening SW. It is suggested that both effects are interrelated.

We do not consider here other possible important effects in this study, which may also change the saturation level of U_{PC} and Ψ, for example, the ionosphere and SW conductivity effects [e.g. *Lyatsky et al.*, 2010; *Kan et al.,* 2010, *Gao et al.*, 2013].

The database and processing methods

We use data of the superstorms: 24 September 1998, 6 April 2000 and 20 November 2003. The main input for the magnetogram inversion technique (MIT) [e.g. *Mishin*, 1990] are data of more than 110 ground magnetometers of the Northern Hemisphere.

Table 1. SW conditions and geomagnetic indexes

Date\ Parameters	AE, nT	SYM-H, nT	Bz, nT	By, nT	P_d, nPa
24-25 Sept. 1998	73 ÷ 2865	≤ -300	-23 ÷ 23	-13 ÷ 39	0.5 ÷ 28
6-7 Aug. 2000	22 ÷ 2000	≤ -300	-30 ÷ 21	-30 ÷ 8	0.7 ÷ 25
20 Nov. 2003	13 ÷ 3250	≤ -450	-53 ÷ 30	-26 ÷ 44	1.5 ÷ 26

Table 1 shows the range of variations of the observed SW parameters and AE index, and also the minimum value of the SYM-H index for the three superstorms above. Abnormally strong values of IMF and P_d caused the appropriate activity of the aurora and ring current: AE-index reached, respectively, ~ 2000, 1750 and 3000 nT, and the latitude of the polar cap boundary lowered to 60^0.

Fig. 1 shows an example of maps of field−aligned currents (FAC) density distribution in the polar ionosphere, obtained by MIT for the 20 November 2003 superstorm. Thick solid lines show the boundaries of the Iijima−Potemra regions R0, R1, R2. The polar cap R0 is inside the region R1. On the basis of such maps we obtained time series $\Psi_1(t)$, where $\Psi_1 = \Psi - \Psi_0$ - is the value of the total open magnetic flux Ψ minus its value before the substorm Ψ_0 = const [*Mishin et al.*, 2014]. The polar cap magnetic flux Ψ in MIT is calculated as a product $\Psi = B \cdot S$, where B=0.6 Gs is the average geomagnetic field in a polar ionosphere, and S is the polar cap area. Further, in MIT the Poynting flux is calculated as a function of the magnetic flux $\varepsilon' \sim (\Psi_1)^2$ through the area of the polar cap S obtained from the FAC maps [*Mishin et al.*, 2014], rather than through the expected unmeasurable length of an reconnection line l_0 at the magnetopause as in the method by Akasofu [*Perreault and Akasofu*, 1978].

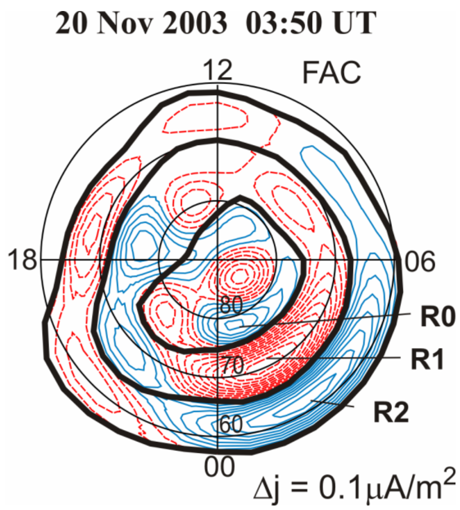

Figure 1. Maps of field-aligned current (FAC) density in the northern high-latitude ionosphere in geomagnetic dipole coordinates (MLT- latitude) obtained by magnetogram inversion technique (MIT) with 1–min resolution. Downward (upward) FACs are shown by dashed (solid) lines), borders between FAC zones R_1, R_2, R_0–by **thick** lines. R_0 – polar cap.

In the global PPMLR- MHD simulation model [*Hu et al.*, 2009; *Wang et al.*, 2014] the basic input data are the SW parameters. The energy flux from SW to the magnetosphere is determined through a normal component of the velocity and magnetic field vectors at the magnetopause and its area. The total energy flux Q_T includes in addition to the Poynting flux Q_{elm} also the thermal and kinetic energy fluxes.

Unlike satellite statistical data averaged over intervals of about an hour, we use the original MIT methods for determining Ψ (with a sampling interval of ≥1 min) [*Mishin et al.*, 2014] and for identifying hidden dependencies of Ψ on the variables E_{sw}, P_d, and AE−index [e.g. *Mishin*, 1990].

The method of maximal contributions

We use this method for a detection and separation in time of hidden dependencies of the open magnetic flux Ψ_1 (E_{sw}, P_d) obtained from observations [e.g. *Mishin*, 1990]. We assumed that the values Ψ_1 are controlled mainly by AE-index values and by the SW parameters E_{sw} and P_d. This method provides solving systems of the linear algebraic equations, including those used in the present paper, having the form:

$$\Psi_i = A_1 \cdot E_i + A_2 \cdot P_i + A_3 \cdot AE_i \qquad (1)$$

where i =1, *k* is the number of each time instant in the time interval considered, k - the quantity of these instants for this interval (their centers are shown by three different symbols in Fig. 3).

The polar cap magnetic flux Ψ1 variation

Fig. 2 shows the saturation of the open magnetic flux Ψ_1, calculated by MIT during the growth of the southward IMF and Pd for the 20 November 2003. superstorm.

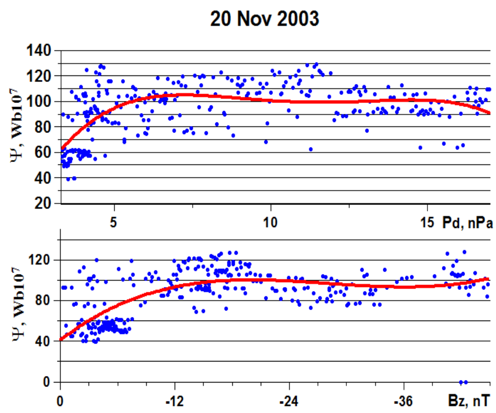

Figure 2. “New” polar magnetic flux $\Psi_{1=}$ Ψ- Ψ_0 as a function of (**a**) the SW dynamic pressure Pd and the IMF B_z (**b**). Here Ψ_0=0.35GWb-the prestorm Ψ value.

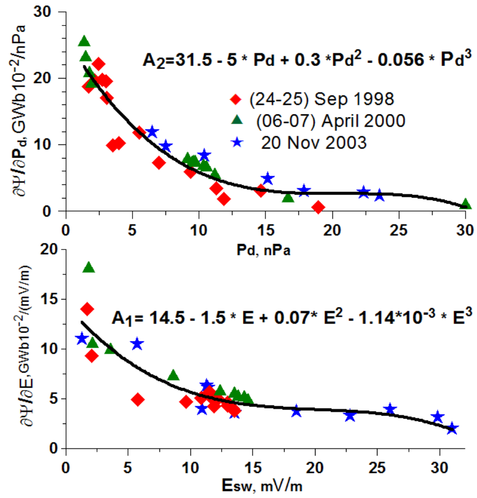

Figure 3. Derivatives ∂Ψ/∂P и ∂Ψ/∂E as a functions of P_d and E_{sw} for the three superstorms.

The dispersion is due to the fact that the flux Ψ_1 is a function of many SW parameters. In order to separate two processes of saturation Ψ_1 (B_z) and Ψ_1 (P_d) in time we have used the method of maximal contributions with short intervals $\Delta x_i \leq 20$ min and obtained a series of derivatives $\partial\Psi / \partial P_d$ and $\partial\Psi / \partial E_{sw}$ depending on P_d and E_{sw}.

Fig. 3 shows graphs of these dependencies, built from three superstorms data. Saturation processes of Ψ_1 (B_z) and Ψ_1 (P_d) are separated in time and can occur independently. Results for the three discussed events fit together and complement each other. The derivatives decrease exponentially when the value E_{sw} and P_d continues to grow, confirming the Ψ_1 saturation effect for the strengthening SW. The SW electric field and the dynamic pressure depend on the SW velocity V_{sw}. In this regard, a question may arise about dependence from each other of parameters P_d and E_{sw}. Fig. 4 on an example of the 20 November 2003 event shows that for the interval (08:45 – 24:00) UT the SW velocity Vsw decreases very slowly. Our analysis has shown that in this interval the field E_{sw} variation is mainly determined by the change of non-radial IMF $B = (By^2 + Bz^2)^{1/2}$ (correlation coefficient Kcor (Esw, B) = 0.87), and the change in P_d - change in the density n (Kcor (Pd, n) = 0.93). Thus the E_{sw} and P_d parameters can be considered independent on the whole interval superstorm (except SSC, when at the same time all the parameters change on the front SW inhomogeneity) and speak about the saturation of the polar cap magnetic flux and the Poynting flux ε' from both of them separately.

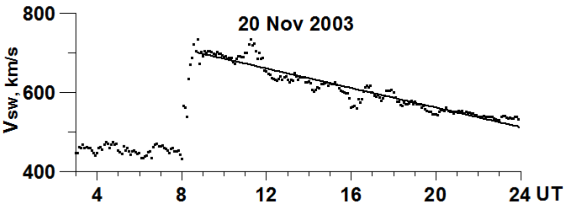

Figure 4. Solar wind velocity variation during the superstorm.

Thus, the MIT results indicate the presence of Ψ saturation under superstorm with continuous increase of not only E_{sw}, but also P_d. Simultaneously with the saturation of Ψ there is slowdown of the Poynting flux ε' from SW to the polar ionosphere.

Poynting flux: Comparison with MHD model

Now we compare the results of MIT and the global PPRML MHD model. For the 20 November 2003 superstorm graphs of variation of a total energy flux and electromagnetic energy flux Q_{elm} (Poynting flux) were calculated by the PPMLR MHD model.

Fig. 5 shows the variation of the only electromagnetic flux Q_{elm}, as its contribution to the total flux Q_{total} amounted to more than 90%. It can be seen that: 1) for small values of P_d <5nPa and IMF Bz> -10nT there is a growth of the power, and its values obtained by two models are close; 2) reaching a maximum at the $P_d \geq$ (12-14) nPa, the Q_{elm} flux does not increase further; 3) an increase in the flux depending on the southward IMF slows when B_z <-30nT and almost stops at values $B_z \leq$-40nT, rarely observed during superstorms. For Bz<-20nT, about half power, transported into the magnetosphere, penetrates into the polar cap ($\varepsilon' \sim 0.5\ Q_{elm}$).

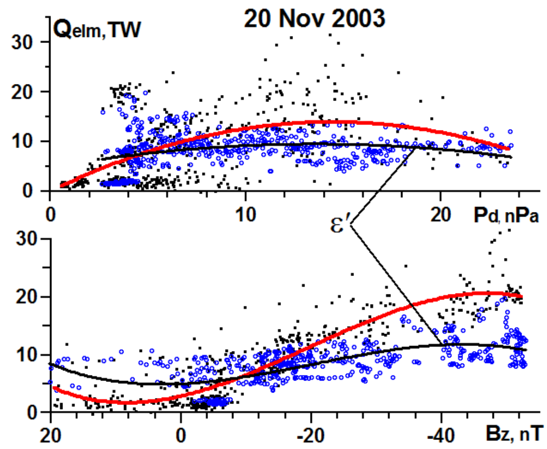

Figure 5. Variations of the Poynting flux: into the magnetosphere - Q_{elm} (black dots and their approximating thick curves, obtained by the MHD model) and into the polar cap $-\varepsilon'$ (circles, thin approximating lines, obtained by MIT) as a function of the dynamic pressure Pd and IMF Bz <0.

On the saturation effect and finite compressibility of the magnetosphere

a) Effect of Pd on the magnetopause position

Reasonably to assume that the displacements of the polar cap boundary and of the magnetopause are interrelated. From the equilibrium condition of the magnetopause - balance of the total pressure $P+B^2/2\mu_0=const$, it is easy to see that its compression with increasing pressure P_d rapidly slows down and under values typical for superstorms practically stops. It means that magnetopause nose position has minimal limit. For compressed dipolar field $B(r) \approx 2B(R_E)/r^3$ to reduce subsolar relative radius $L / L_0 = r_{mp}/R_0$ ($R_0 \approx 10R_E$) from 10 to 5 (i.e. half) it is necessary to overcome geomagnetic pressure $P_{BE}(r) \sim 1/r^6$, i.e. to increase P_d in 2^6=64 times. Fig. 6 show very slow magnetopause inward motion for $P_d / P_{BE}(r_0)>10$.

b) Effect of the southward IMF

If we following to *Kovner and Feldstein* [1972], assume that the southward IMF penetrates by diffusion inside the magnetopause and reduce geomagnetic field, it also results in the dayside magnetopause inward movement to restore the pressure balance (another possible reason is the negative feedback effect of the Region1 FACs on the B_E value at the dayside magnetosphere [*Maltsev and Lyatsky*, 1975; *Sibeck et al.*, 1991; *Siscoe et al.*, 2002]). But it is also easy to see, that the compression of the magnetosphere decelerates quickly at the amplification of both P_d and negative IMF Bz. Analogical behavior is seen for the polar cap magnetic flux Ψ. Fig. 6 shows that for the powerful superstorm, saturation effect–a growth slowing occurs since values B_z < -30 nT and P_d>10 nPa.

Thus, even for stronger superstorm SW parameters, it is practically impossible to compress the magnetosphere more than twice. That is why there must be an upper limit of the magnetic flux transfer into the polar cap.

The MHD model calculations for steady conditions made for the B_z values from B_z= -5 nT to B_z= -20 nT, gave a permanent L_{mp} decrease and Q_{el} growth with no signs of a saturation. This is contrary to the actual observed saturation of U_{PC} and Ψ [e.g. *Lopez et al.*, 2007; *Borovsky et al.*, 2009].

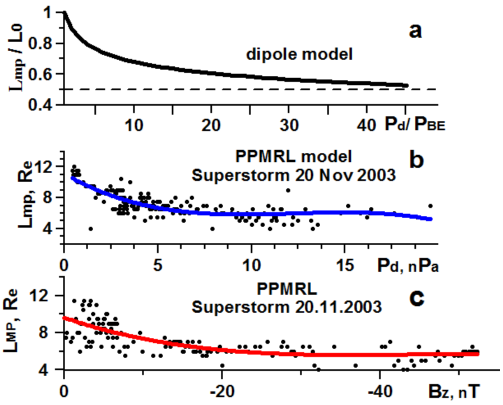

Figure 6. (**a**) Dipole model: the relative subsolar magnetopause distance as a function of the relative SW pressure Pd/ $P_{BE}(r_0)$ changing from 1 up to value 2^6, when L/L_0=1/2. (**b, c**) MHD model: L_{mp} as a function of P_d (**b**) and B_z (**c**) during the superstorm. Solid line–approximating curve.

Possible reasons for this are rather long period (several hours) required to meet the steady condition, that for the actual conditions during superstorms is not realized; and that the real saturation level is below Bz_{min}=-20 nT and was not achieved.

Conclusions

Comparison of variations of the Poynting flux into the magnetosphere obtained by MIT and the MHD model for the 20 November 2003 event, has shown:

− In the initial phase of the storm, when the P_d and southward IMF values were small (P_d <4 nPa, B_z < -5 nT), input power values were almost the same;

− With the increasing of P_d and southward IMF, there is a growth of the Poynting flux. This growth begins to slow down when P_d ~ (5÷8), and when P_d> 14 nPa it stops; the Poynting flux increase depending on the southward IMF slows down when B_z < -20nT and almost stops at $B_z \leq$ -40nT, rarely observed for superstorms, while about half of the power transferred into the magnetosphere gets into the polar cap (ε′ ~ 0.5 Q_{elm}).

We assume that the saturation effect of the Ψ and Poynting fluxes are associated with the slowing of both the magnetosphere compression and the polar cap expansion at significant SW strengthening.

The PPMLR–MHD model shows the saturation effect for superstorm conditions, but does not show it in steady conditions for Bz > -20nT.

Acknowledgments. The AE index was obtained through the WDC Website, Kyoto, magnetic data from the CANOPUS, INTERMAGNET, GIMA, MACCS, IMAGE and SuperDARN international projects, from magnetic networks in Arctic and the Antarctic (the Shafer Institute of Cosmo-Physical Research and Aeronomy SBRAS, Arctic and Antarctic Research Institute, and DMI), and individual magnetic observatories. Study is supported by RFBR Grants 14-05-91165 and 15-05-05561, C. Wang is supported by the NSFC grant 413111039

References

Borovsky J.E., B. Lavraud and M. Kuznetsova. Polar cap potential saturation, dayside reconnection, and changes to the magnetosphere// J. Geophys. Res. **114.** A03224, doi:10.1029/2009JA014058. 2009

Gao Y., M.G. Kivelson, and R.J. Walker. Two models of cross polar cap potential saturation compared: Siscoe - Hill model versus Kivelson-Ridley model// J. Geophys. Res. **118.** 794–803. doi:10.1002/jgra.50124. 2013

Hu Y.Q., Z. Peng, C. Wang, and J. R. Kan. Magnetic merging line and reconnection voltage versus IMF clock angle: Results from global MHD simulations//J. Geophys. Res. **114**. A08220. doi:10.1029/2009JA014118. 2009

Kan J.R., H. Li, C. Wang, B.B. Tang, and Y.Q. Hu. Saturation of polar cap potential: Nonlinearity in quasi-steady solar wind-magnetosphere-ionosphere coupling//J. Geophys. Res. **115**. A08226. doi:10.1029/2009JA014389. 2010

Karavaev Yu.A., A.A. Shapovalova, V.M. Mishin and V.V. Mishin (a). Superstorm on 20.11.2003: identification of hidden dependencies of the tail lobe magnetic flux on the solar wind dynamic pressure// Proc. of the 9-th Intern. Conference "Problems of Geocosmos" (St. Petersburg, Russia, 8-12 October 2012). St. Petersburg State University. 2012. 245-250

Karavaev Yu.A. et al.(b). Superstorm (24-25) 09.1998: identification of hidden dependencies of the tail lobe magnetic flux on the solar wind dynamic pressure// ibid: P. 251-255

Kovner M.S. and Ya.I. Feldstein. On solar wind interaction with the Earth's magnetosphere//Planet. Space Sci. **21**. 1191-1211. 1973.

Lopez R.E., J.G. Lyon, E. Mitchell et al. Why doesn't the ring current injection rate saturate? // J. Geophys. Res. **114**. A02204. doi:10.1029/2008JA013141. 2009

Lyatsky W., G.V. Khazanov, and J.A. Slavin. Saturation of the electric field transmitted to the magnetosphere//J. Geophys, Res. **115**. A08221, doi:10.1029/2009JA015091. 2010

Maltsev Yu.P and, W.B. Lyatsky. Field-aligned currents and erosion of dayside magnetosphere// Planet. Space Sci. **23**.1257-1261.1975

Merkin V.G. and C.C. Goodrich. Does the polar cap area saturate? //Geophys. Res. Lett. **34**, L09107, doi:10.1029/2007GL029357. 2007

Mishin V.M. The magnetogram inversion technique and some applications//Space Sci. Rev. **53**(1). 83-163. 1990

Mishin V.V., V.M. Mishin, Z. Pu et al. Old tail lobes effect on the solar-wind - magnetosphere energy transport for the 27 August 2001 substorm // J. Adv. Space. Res. 2014. **54**(12). 2540-2548

Perreault P. and S-I. Akasofu. A study of geomagnetic storms//Geophys. J. R. Astr. Soc. **54.** 547-573. 1978

Sibeck D., R. Lopez, and E. Roelof. Solar wind control of the magnetopause shape, location, and motion// J. Geophys. Res. V. 96. P. 5489–5495. 1991.

Siscoe G. L., N.U. Crooker, and K.D. Siebert. Transpolar potential saturation: Roles of region 1 current system and solar wind ram pressure//J. Geophys. Res. **107.** 1321. doi:10.1029/2001JA009176. 2002.